Thermodynamics of fluids obtained by mapping the collision properties

Alejandro Gil-Villegas* and Fernando del Río†
Departamento de Física, Universidad Autónoma Metropolitana, Iztapalapa, Apartado postal 55-534, 09340 México Distrito Federal, Mexico

Carlos Vega
Departamento de Química-Física, Facultad de Ciencias Químicas, Universidad Complutense de Madrid, 28040 Madrid, Spain
(Received 17 October 1994)

A method for deriving theoretical relations for thermodynamic properties of simple model fluids is developed. The method uses mean collision properties to write the thermodynamics of a system in terms of the equation of state of an equivalent system used as reference. The equivalent fluid is formed by particles interacting with a square-well (SW) potential whose properties are known accurately. The equivalence to the SW fluid is made by means of mapping equations for the SW potential parameters. Solution of the mapping equations at a few state points plus the use of simple parametric equations for the SW potential parameters allows us to write the equation of state (EOS) of the fluid. The EOS derived by this method illuminates the relation between thermodynamic properties of the fluid and relevant features of the intermolecular potential, and gives reliable predictions of the thermodynamics including the liquid-vapor equilibrium. This is tested by obtaining the EOS of the Lennard-Jones fluid and comparing it with very accurate empirical EOS available for this system. The EOS for fluids with a commonly used interaction potential (EXP6) are derived and used to discuss the liquid-vapor equilibria of these systems, with the particular attention to deviations from corresponding-state behavior.

PACS number(s): 61.20.−p, 05.70.Ce, 64.10.+h

I. INTRODUCTION

An important problem in the thermodynamics of fluids is to derive analytical equations of state (EOS) for real substances, i.e., to obtain explicit relations for the thermodynamic variables in terms of relevant molecular features. Such relations allow us to understand the specific behavior of a real substance in terms of its molecular features and, on practical terms, to use efficiently the usually limited knowledge of the properties of a substance to predict their values in other states. As far as this goal has not been fully attained, the practical need of EOS has produced alternative and less ambitious approaches. The most direct is the fit of empirical functions to experimental data of a specific fluid. These empirical equations involve many parameters and require extensive experimental data over wide ranges of pressure and temperature as, for example, in the Benedict-Webb-Rubin and Strobridge equations [1,2]. These empirical EOS are specific to a substance, and their parameters lack of a physical meaning. An alternative approach is provided by semiempirical equations, e.g., those of Redlich-Kwong, Peng-Robinson, or Soave [3–5]. These EOS are widely used in engineering applications and require less experimental information to determine the parameters. In many cases the semiempirical equations are modifications of the van der Waals (vdW) equation. Both empirical and semiempirical EOS share two problems: there is no sure way to improve their accuracy, and their parameters are not rigorously related to molecular properties. In contrast, approaches based on statistical mechanics, although not as straightforward, provide a physical understanding of the thermodynamics and are potentially of very high accuracy.

The statistical-mechanical approach assumes a model for the intermolecular potential $u(r)$, and uses some method (computer simulations, integral equations, perturbations, etc.) to calculate the thermodynamics either directly or by means of the radial distribution function $g(r)$. After decades of development, these methods allow us to determine $g(r)$ and the thermodynamics with very good accuracy for various models of the intermolecular potential, and more refined techniques promise higher accuracy and wider applicability. However, all these methods, except for a few important but not very realistic potentials, provide only numerical information for each specific model of $u(r)$ assumed. Here the question of deriving analytic equations of state is still open. From the theoretical viewpoint the aim is to relate explicitly the thermodynamic properties of the fluid to relevant molecular features of the potential $u(r)$. In the practical side, solution of this problem would extend the reliability and predictive potential of EOS. In this paper we develop a systematic procedure to obtain theoretical and analytic equations of state from model potentials by using statistical mechanics.

Recently [6] we suggested a way to derive EOS for a

*Present address: Department of Chemistry, The University of Sheffield, Sheffield, U.K.
†Author to whom correspondence should be addressed.

simple model potential by means of collision concepts [7,8] and perturbation theory. In the present work we give a formal and rigorous basis for the theory and extend it to obtain accurate EOS for simple realistic systems. The basis ideas of the method are as follows. For a fluid with intermolecular potential $u(r)$ two collision quantities are introduced: the mean diameter $\langle s \rangle$ and the mean range $\langle l \rangle$; both are functionals of $u(r)$ and depend on density $\rho = N/V$ and temperature T. These collision properties are then used to determine an equivalent square-well (SW) system in such a way that the pressures of both systems are equal. The collision parameters of the equivalent SW fluid, a diameter σ and an attractive range λ, are determined at each temperature and density, so that for any state (ρ, T) one finds an equivalent SW system with parameters $\sigma(\rho, T)$ and $\lambda(\rho, T)$. The original system in a given state is hence mapped into a particular SW system, whose equation of state is very well known [9-12]. As to the apparently privileged use of the SW system, it can be shown that the thermodynamic mapping can be done into reference systems different from the SW, such as the Yukawa fluid. However, the use of other equivalent fluids lays beyond the scope of this work.

This method is based on statistical mechanics and kinetic theory, and is in principle exact, i.e., it provides theoretical equations of state which can be systematically improved in accuracy. It can also be extended to more complex situations, like molecular fluids, mixtures and inhomogeneous fluids; nevertheless, this paper is devoted to pure fluids and spherically symmetric $u(r)$. The aim of the method is similar to those of other fluid theories using different approaches [13-22]; some of these, like the work of Aim and Nezbeda [13-15], although are less rigorous, also use the idea of an equivalent system.

In this paper we formally develop a rigorous basis for the theory and apply it to various systems and problems, improving on approximations used in the preliminary scheme. First, the concept of mapping between equivalent thermodynamic systems is introduced and used to develop and discuss a theory for the equation of state. Second, the reliability of the applications is increased by using accurate values for $g(r)$ based on the reference-hypernetted-chain (RHNC) integral equation in its modern version [23–27]. An accurate treatment of the structure extends the applicability of the theory to very dense fluids, avoiding problems of multiple and nonphysical solutions. Third, we illustrate the application of the theory in two cases: the well-known Lennard-Jones fluid, for which many results are available for comparison, and the family of EXP6 potential models for which no analytical equations of state have been previously developed.

Perhaps the main theoretical virtue of the method is that the EOS parameters acquire a clear physical meaning and hence illuminate the relation between the microscopic and thermodynamic levels, e.g., in the understanding of deviations from the principle of corresponding states. The most important practical advantage of the method proposed here is that reliable and analytical EOS for model fluids are obtained from the knowledge of their properties at a few state points.

Section II addresses the basic concepts of the theory. Section III discusses the main features of the theory, and briefly reviews the techniques used to determine the properties of the reference SW fluid and of the systems of interest. In Sec. IV the Lennard-Jones (LJ) case is presented as an illustrative test, and EOS of EXP6 fluids are derived. These EOS are used to predict the liquid-vapor equilibrium of EXP6 fluids (the EXP6 potential is defined below). Finally, the main conclusions of this work are stated.

II. THEORY

A. Equivalent fluids and mapping equations

Let us consider a classical fluid system, denoted by Ψ, whose particles interact through the pair potential $u(r)$, and another system Ψ_0, to be called the reference system, with interaction potential $u_0(r)$. The potential $u(r)$ is assumed to be spherically symmetric and of realistic shape: it has its minimum $u(r_m,) = -\varepsilon$ at $r = r_m$, is repulsive for $r < r_m$ and attractive for longer distances. The reference potential $u_0(r)$ is spherical and also includes repulsive and attractive forces. By reference "system" we will really mean a *family* $\{\Psi_0\}$ of systems whose potentials $u_0(r;\varepsilon_0,\alpha,\xi)$ all have the same functional dependence on r through three parameters ε_0, α, and ξ, where ε_0 is the value of $u_0(r)$ at its minimum, and α and ξ are required for a full description of $u_0(r)$. For instance, if $\{\Psi_0\}$ is the SW family with interparticle potentials given by

$$u_{\mathrm{SW}} = \begin{cases} \infty, & r \le \sigma_{\mathrm{SW}} \\ -\varepsilon_0, & \sigma_{\mathrm{SW}} \le r \le \lambda\sigma_{\mathrm{SW}} \\ 0, & r \ge \lambda\sigma_{\mathrm{SW}} , \end{cases}$$

then $\alpha = \sigma_{\mathrm{SW}}$ is the hard-core diameter and $\xi = \lambda\sigma_{\mathrm{SW}}$ is the distance beyond which the potential vanishes. In this case, the reference family $\{\Psi_0\}$ of SW fluids is obtained by varying the range λ.

We also assume that the properties of $\{\Psi\}$ are well known, in particular the equation for its pressure $P_0(\rho, T)$ or compressibility factor $\beta P_0/\rho = Z_0(\rho, T)$, with $\beta = 1/kT$. Z_0 depends both on the state and on the parameters ε_0, α, and ξ, i.e., $Z_0(\rho, T; [u_0]) = Z_0(\rho, T; \varepsilon_0, \alpha, \xi)$. Then we ask whether the properties of Ψ can be written in terms of the reference $\{\Psi_0\}$. (This question is easily answered in the trivial case when Ψ and Ψ_0 follow the principle of corresponding states, and perturbation theory shows how to relate both systems, but only in an approximate way.)

In order to determine the system Ψ_0 equivalent to Ψ at a given ρ and T, we impose that the pressures of Ψ and Ψ_0 be equal, i.e.,

$$Z(\rho, T; [u]) = Z_0(\rho, T, \varepsilon_0, \alpha, \xi) . \tag{1}$$

This relation is an implicit equation for the reference parameters ε_0, α, and ξ. In general, as long as $\{\Psi_0\}$ is chosen conveniently, Eq. (1) will have many solutions at the given ρ and T: there will be many combinations of values for these parameters giving the same pressure in both systems. In order to determine uniquely the

equivalent system Ψ_0, one needs to impose extra conditions. We now show how this can be done by means of kinetic arguments.

Using kinetic theory, the compressibility factor of Ψ may be written as [7,8]

$$Z=1+\frac{2}{3\nu_r}[\langle s\rangle\nu_R-\langle l\rangle\nu_A] , \tag{2}$$

where $\nu_r=4(kT/\pi m)^{1/2}$ is the mean relative velocity and m is the mass of a particle. Equation (2) can be obtained from the kinetic derivation of the virial theorem by separating the contributions of repulsive and attractive forces to the total pressure. The quantities $\langle s\rangle$ and $\langle l\rangle$ are, respectively, the mean distances at which elastic repulsive and attractive collisions occur. The frequencies ν_R and ν_A are the number of repulsive and attractive collisions per unit time, respectively. The main value of Eq. (2) is the neat separation of repulsions and attractions: the term $\langle s\rangle\nu_R$ gives the effect of repulsive collisions, proportional to the repulsive contribution to the pressure, whereas $\langle l\rangle\nu_A$ is proportional to the attractive pressure. In equilibrium, these quantities are determined from the differential collision frequency $\mu(r)$ by the expressions [8]

$$\langle s\rangle=\frac{1}{\nu_R}\int_0^{r_m} s\mu(s)ds , \tag{3}$$

$$\langle l\rangle=\frac{1}{\nu_A}\int_{r_m}^{\infty} l\mu(l)dl , \tag{4}$$

$$\nu_R=\int_0^{r_m}\mu(l)dl , \tag{5}$$

$$\nu_A=\int_{r_m}^{\infty}\mu(l)dl , \tag{6}$$

where $\mu(r)$, the number of collisions in $(r,r+dr)$ per unit distance and unit time, is

$$\mu(r)=\pm\pi\rho\nu_r r^2 y(r)\partial[\exp(-\beta u(r))]/\partial r , \tag{7}$$

with the sign chosen so that $\mu(r)\geq 0$ and $y(r)=g(r)\exp(-u)$. Due to (7), in order to evaluate $\langle s\rangle$, $\langle l\rangle$, ν_R, and ν_A, one needs the radial distribution function $g(r)$ of Ψ.

The compressibility factor of Ψ_0 takes a form similar to (2):

$$Z_0=1+\frac{2}{3\nu_{r0}}[\langle s\rangle^0\nu_R^0-\langle l\rangle^0\nu_A^0] . \tag{8}$$

Assuming the reference particles of the same mass m, then $\nu_{r0}=\nu_r$. All the collision quantities in (8) depend on the potential parameters ε_0, α, and ξ.

We now propose the conditions necessary to determine Ψ_0. First, we take the depths of the potentials $u(r)$ and $u_0(r)$ to be equal:

$$\varepsilon=\varepsilon_0 , \tag{9}$$

and, second, impose the equality between the repulsive contributions of Ψ and Ψ_0 to the pressure, and, separately, between the attractive contributions. Writing these conditions in terms of the collision quantities,

$$\langle s\rangle\nu_R=\langle s\rangle^0\nu_R^0 , \tag{10a}$$

$$\langle l\rangle\nu_A=\langle l\rangle^0\nu_A^0 . \tag{10b}$$

Since ε_0 is simply fixed by (9), Eqs. (10) constitute a set of coupled equations for the two remaining unknowns α and ξ. Moreover, the equality of pressures, Eq. (1), is recovered by adding (10a) to (10b) and using (2) and (8). To illustrate with a concrete example, if Ψ is the Lennard-Jones system with potential

$$u_{\rm LJ}(r)=4\varepsilon_{\rm LJ}[(\sigma_{\rm LJ}/r)^{12}-(\sigma_{\rm LJ}/r)^6] ,$$

and $\{\Psi_0\}$ is the family of SW systems with variable range, we look for the particular SW so that the repulsive and attractive pressures are the same in both the LJ and SW fluids at a given ρ and T. Provided that $\varepsilon_{\rm LJ}=\varepsilon_0$, Eqs. (10) will hold only when an adequate choice of $\sigma_{\rm SW}$ and λ is made.

In order to solve Eqs. (10), one needs the functions $g(r)$ and $g_0(r)$ for the systems Ψ and Ψ_0. Moreover, an iterative procedure is required because the collision frequencies and parameters of Ψ_0, on the right-hand sides of (10), depend in a nontrivial way on the potential parameters α and ξ.

Equations (9) and (10) relate the system Ψ, at a given ρ and T, with one system of $\{\Psi_0\}$ identified by particular values of ε_0, α, and ξ. Therefore, (9) and (10) define a mapping $\Psi\rightarrow\{\Psi_0\}$ between the system with potential $u(r)$ and a the reference systems with $u_0(r)$. Solution of the *mapping equations* (9) and (10) for ε_0, α, and ξ, must be carried out at every ρ and T of interest. The mapping here proposed is such that the repulsive and attractive contributions to the pressure are kept the same in Ψ_0 as in Ψ.

Let us briefly discuss why a full family $\{\Psi_0\}$ is necessary for the mapping, i.e., why it is usually not enough to consider a single constant reference system. In the latter case, the potential parameters α and ξ, obtained from the mapping equations, will be independent of ρ and T, so that the pressures of Ψ and Ψ_0 are equal at all state points. This simple behavior occurs only when Ψ and Ψ_0 follow the principle of corresponding states, i.e., when $u(r)$ and $u_0(r)$ are conformal. But, in general, different parameters α and ξ are needed at different states. Take the case of two similar fluids, such as the LJ fluid and the SW fluid with $\sigma_{\rm SW}=\sigma_{\rm LJ}$ and $\lambda=1.5$. This similarity would be exact only if Eqs. (10) have the same solution $\alpha=\sigma_{\rm LJ}=\sigma_{\rm SW}$, and $\xi=\lambda\sigma_{\rm SW}=1.5\sigma_{\rm SW}$ at all ρ and T. But the actual solution of the mapping equations shows that this is not true, for the LJ and SW potentials are not conformal. It is difficult to establish *a priori* the particulars of the dependence of α and ξ on ρ and T, but it will measure the deviations from strict corresponding-state behavior for the potentials $u(r)$ and $u_0(r)$.

B. SW as reference fluid

In the rest of this paper we shall choose the square-well system as the reference family $\{\Psi_0\}$. With this choice the collision frequencies and parameters $\langle s\rangle^{\rm SW}$ and $\langle l\rangle^{\rm SW}$

are given by [7,10]

$$\langle s \rangle^{SW} = \sigma_{SW} , \tag{11a}$$

$$\langle l \rangle^{SW} = \lambda \sigma_{SW} , \tag{11b}$$

$$\nu_R^{SW} = \pi \rho \nu_r \sigma_{SW}^2 \nu_{SW}(\sigma_{SW}) e^{\beta\varepsilon} , \tag{11c}$$

$$\nu_A^{SW} = \pi \rho \nu_r (\lambda \sigma_{SW})^2 y_{SW}(\lambda \sigma_{SW})(e^{\beta\varepsilon} - 1) . \tag{11d}$$

It is clear from these equations and (1) that knowledge of $y_{SW}(\sigma_{SW})$ and $y_{SW}(\lambda\sigma_{SW})$ is sufficient to determine all the collision parameters and the pressure of the system. For the SW reference (11) and using (9), the mapping equations (10) become explicitly

$$\sigma_{SW}^3(\rho,T) y_{SW}(\sigma_{SW}) e^{\beta\varepsilon} = \int_0^{r_m} ds\, s^3 y(s) \frac{\partial \exp[-\beta u(s)]}{\partial s} , \tag{12a}$$

$$\lambda^3(\rho,T)\sigma_{SW}^3(\rho,T) y_{SW}(\lambda\sigma_{SW})(e^{\beta\varepsilon} - 1) = -\int_{r_m}^{\infty} dl\, l^3 y(l) \frac{\partial \exp[-\beta u(l)]}{\partial l} . \tag{12b}$$

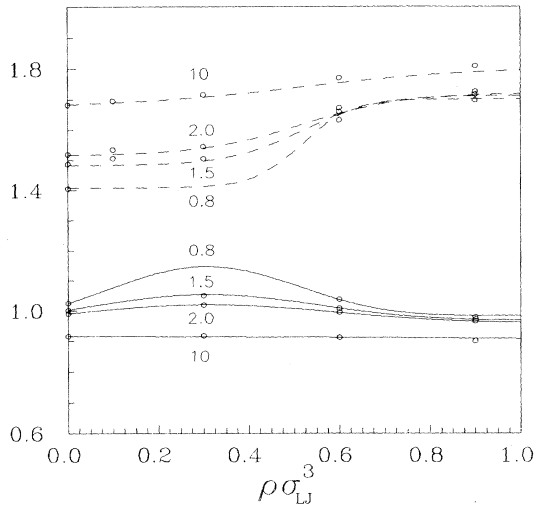

FIG. 1. Equivalent SW diameter σ_{SW} (solid lines) and range λ (dashed lines) of the Lennard-Jones fluid as a function of density. The circles show direct results from the mapping equations and the RHNC equation. The lines labeled by the temperature $T^* = kT/\varepsilon$ stand for the parametric equations (19).

III. SOLUTION OF THE SW MAPPING

A. General features of the mapping method

The mapping equations (12) are solved by iteration given a procedure to determine $y_{SW}(\sigma_{SW})$, $y_{SW}(\lambda\sigma_{SW})$, and $g(r)$ for the system of interest. We start by analyzing the general features of the mapping method with a concrete example in view. Table I and Fig. 1 present the results of mapping the LJ fluid into the SW reference at various states. The parameters $\alpha = \sigma_{SW}$ and $\xi = \lambda\sigma_{SW}$ are shown for different states, e.g., the second row indicates that a LJ fluid at $T^* = kT/\varepsilon_{LJ} = 0.8$ and $\rho^* = \rho\sigma_{LJ}^3 = 0.9$ has the same repulsive and attractive pressures as a SW fluid, at the same ρ and T, with $\sigma_{SW} = 0.977\,42$ and $\lambda = 1.697\,12$. In SW reduced units, $\rho_{SW}^* = \rho\sigma_{SW}^3 = 0.8404$.

TABLE I. Square-well collision parameters of the Lennard-Jones fluid from the RHNC theory.

T^*	$\rho\sigma_{LJ}^3$	σ_{SW}/σ_{LJ}	λ	$\rho\sigma_{SW}^3$
0.80	0.00	1.020 53	1.405 52	0.0000
0.80	0.90	0.977 42	1.697 12	0.8404
1.50	0.00	1.002 14	1.487 04	0.0000
1.50	0.30	1.050 45	1.504 73	0.3477
1.50	0.60	1.006 97	1.659 23	0.6126
1.50	0.90	0.970 36	1.716 18	0.8223
2.00	0.00	0.990 65	1.519 34	0.0000
2.00	0.30	1.019 20	1.544 58	0.3176
2.00	0.60	0.993 89	1.671 59	0.5891
2.00	0.90	0.964 15	1.726 14	0.8066
10.0	0.00	0.916 25	1.682 90	0.0000
10.0	0.30	0.917 69	1.694 96	0.2319
10.0	0.60	0.911 30	1.770 28	0.5468
10.0	0.90	0.900 17	1.809 88	0.6565

As expected, both σ_{SW} and λ depend on ρ and T.

The mapping method requires us to evaluate $g(r)$ of both systems Ψ and Ψ_0 (the SW in our case). Calculation of $y_{SW}(\sigma_{SW})$ and $y_{SW}(\lambda\sigma_{SW})$ is not a problem. First, as shown below, from the Helmholtz free-energy function of the SW system $A_{SW}(\rho,T,\lambda)$, one can immediately derive all the thermodynamic and structural information required by the mapping equations. Second, accurate knowledge of $A_{SW}(\rho,T,\lambda)$ is currently available. On the other hand, $g(r)$ can be calculated either by simulations—Monte Carlo (MC) or molecular dynamics—or by solving the Ornstein-Zernike (OZ) equation with the reference-hypernetted-chain (RHNC) closure. The latter is more economical and has been shown to provide very accurate $g(r)$ of spherical potentials [27-29]. Hence, at least for spherically symmetric $u(r)$, solution of the mapping equations is straightforward. Now, since the pressure may be evaluated directly once $g(r)$ is known, we must discuss the theoretical and practical advantages of the mapping method over direct integration [30].

Direct integration of $g(r)$ determines $Z(\rho,T)$ only at the stages where $g(r)$ is known. As an example of the direct approach to EOS we can mention the work of Johnson, Zollweg, and Gubbins [31], who performed simulations for the LJ system and obtained Z in about 200 states. An empirical EOS (Benedict-Webb-Rubin) containing 35 parameters was then fitted by the least squares method to their results. This Johnson-Zollweg-Gubbins (JZG) EOS is the most accurate thus far available for the LJ fluid. In any direct method like this one needs to perform simulations or solve the RHNC integral equation in a large number of states, and further, the EOS parameters lack any physical meaning.

In the mapping method, the EOS parameters are the collision quantities σ_{SW} and λ which have physical meaning. Hence, when applying the mapping method to different realistic potentials—such as the $n/12$ LJ, the EXP6, or the spherical Kihara families—the behavior of σ_{SW} and λ with ρ and T is very similar to that shown in Fig. 1 (see Figs. 5 and 6, which correspond to two different EXP6 fluids). In fact, the ratio of $\sigma_{SW}(\rho,T)$ of one system to $\sigma_{SW}(\rho,T)$ of another system, and the ratio of the corresponding λ's, measure the deviations from corresponding-state behavior. These ratios play the role of the so-called "shape factors" used in empirical generalizations of the principle of corresponding states [32]. Hence the mapping method gives physical insight into differences in thermodynamic behavior.

Further, the smooth and general behavior of the collision parameters allow us to propose general parametric forms for σ_{SW} and λ. The parameters in these forms are obtained directly, without a least squares method, by solving the mapping equations at only a *few* state points. The parametric expressions are then just substituted into the well-known $Z_{SW}(\rho,T)$ to obtain an analytical expression for the pressure. This means significant savings in computing time over the direct method involving empirical EOS. These features will be developed and used in Sec. III B.

B. Solution of the mapping equations

Solution of the mapping (12) requires the values of $y_{SW}(\sigma_{SW})$ and $y_{SW}(\lambda\sigma_{SW})$. To write Z from Eq. (1), one also needs an equation of state for the SW system Z_{SW}. An accurate equation for the free energy of the SW system, $A_{SW}(\rho,T,\lambda)$, has recently been derived [11,12] and is described in Appendix B. Using this equation,

$$Z_{SW}=\rho(\partial a_{SW}/\partial\rho)\ , \tag{13}$$

where $a_{SW}=\beta A_{SW}/N$. Moreover, $y_{SW}(\lambda\sigma_{SW})$ is given by the exact relation [33]

$$y_{SW}(\lambda\sigma_{SW})\lambda^2(e^{\beta\varepsilon}-1)=-\frac{1}{12\eta}\left[\frac{\partial a_{SW}}{\partial\lambda}\right]_{T,\rho}\ , \tag{14}$$

where $\eta=\pi\rho\sigma_{SW}^3/6$ is the SW packing fraction. Finally, $y_{SW}(\sigma_{SW})$ is found by requiring consistency between Z_{SW} obtained from the free energy, Eq. (13), and that calculated from Clausius's virial theorem (8):

$$Z_{SW}=1+4\eta[y_{SW}(\sigma_{SW})e^{\beta\varepsilon}-\lambda^3 y_{SW}(\lambda\sigma_{SW})(e^{\beta\varepsilon}-1)]\ ,$$

which leads to

$$y_{SW}(\sigma_{SW})=e^{-\beta\varepsilon}[(Z_{SW}-1)/4\eta+\lambda^3 y_{SW}(\lambda\sigma_{SW})(e^{\beta\varepsilon}-1)]\ , \tag{15}$$

and whose right-hand side is given by (13) and (14). It is clear from Eqs. (13)–(15) that all the information required to perform the mapping into the SW system is contained in the free energy function $A_{SW}(\rho,T,\lambda)$.

The function $g(r)$ for $u(r)$ has to be calculated once at each state point, because on iteration only the SW parameters vary. This was done by solving the OZ equation

$$h(\mathbf{r})-c(\mathbf{r})=\rho\int d\mathbf{r}'h(\mathbf{r}')c(|\mathbf{r}-\mathbf{r}'|)\ , \tag{16}$$

with the RHNC closure

$$g(r)=\exp[-\beta u(r)+h(r)-c(r)+B_{HS}(r;d_{HS})]\ . \tag{17}$$

This closure requires the bridge function $B_{HS}(r,d_{HS})$ of hard spheres, which was taken in the parametric form proposed by Malijevský and Labik [26]. The hard-sphere diameter d_{HS} used in (17) is obtained from the equation proposed by Lado [24]:

$$\int d^3r\, d_{HS}[g(r)-g_{HS}(r;d_{HS})][\partial B_{HS}(r;d_{HS})/\partial d_{HS}]=0 \tag{18}$$

together with the Verlet-Weis method to compute $g_{HS}(r)$. Equations (16), (17), and (18) were solved numerically by the procedure proposed by Labik, Malijekský, and Vonka [28].

C. General form of the collision parameters

The values of σ_{SW} and λ obtained from (12) are used to determine two parametric expressions here proposed for $\sigma_{SW}(\rho,T)$ and $\lambda(\rho,T)$. The behavior of $\sigma_{SW}(\rho,T)$ and $\lambda(\rho,T)$ shown in Fig. 1 is quite general for different potentials, and can be adequately represented by

$$\sigma_{SW}^{*3}=\frac{c_0+c_1\exp[-c_2(\rho^*-\omega_1)^2]}{1+c_3\rho^*} \tag{19a}$$

and

$$\lambda=\alpha_0+\alpha_1\tanh[\alpha_2(\rho^*-\omega_2)]\ , \tag{19b}$$

where ω_1 and ω_2 are constants. At constant T, (19a) depends on four parameters, c_i, and (19b) on three, α_i. These parameters are obtained algebraically, without any least squares fitting, from the values of σ_{SW} and λ at only three densities—plus their low-density values which do not involve $g(r)$; see Appendix A for details. Once c_i and α_i are determined at each of four selected temperatures, their T dependence is represented by polynomials in T or $1/T$. The lines in Fig. 1 show σ_{SW}^3 and λ given by (19) for the LJ fluid. The agreement between Eqs. (19) and the values calculated directly from the mapping equations is very good. The required EOS are finally obtained by substitution of (19) for σ_{SW} and λ in EOS of a variable-width SW fluid,

$$Z(\rho,T)=Z_{SW}(\rho\sigma_{SW}^3(\rho,T),kT/\varepsilon,\lambda(\rho,T))\ . \tag{20}$$

In this theory, Z_{SW} is a universal component of EOS, and for a particular fluid one needs the parameters in Eqs. (19). The procedure requires calculating $g(r)$ only at 12 states. Solving for σ_{SW} and λ at more states and using improved parametric equations can systematically increase the accuracy of the resulting EOS.

IV. RESULTS AND DISCUSSION

The mapping equations have been solved for the LJ and two EXP6 potentials. Besides the 12 state points required for the parametrization in Eq. (19), other one-phase states were explored. For the potentials tested, unique solutions of the mapping equations were found in the whole one-phase range up to high densities $\rho^* \approx 1$. In, or near, the liquid-vapor coexistence the RHNC procedure breaks down and the right-hand side of the mapping Eqs. (12) cannot be evaluated.

A. Test with the Lennard-Jones system

The well-known LJ fluid was used to test the mapping method. First, we discuss the behavior of σ_{SW} and λ shown in Fig. 1. The values of the two-phase region are generated by Eqs. (19), and are interpolations of the low- and high-density solutions of the mapping equations. The diameter σ_{SW} depends weakly on ρ at constant T, except close to or below T_c, but depends strongly on T at constant ρ. At high T, σ_{SW} decreases almost monotonically with ρ and in all cases decreases with increasing T. These tendencies follow the expected behavior of the mean collision diameter, and are due to the softness of the core of $u(r)$, as has been shown for purely repulsive systems [34]. The more familiar diameters of the Weeks-Chandler-Andersen (WCA) perturbation theory have a similar behavior [35]. The attractive range λ depends strongly on ρ and T due to the softness of the attractive well. At a given temperature, λ is almost constant at low densities, and increases at high densities.

The theoretical equations of state (TEOS) are given by (20), with the SW EOS described in Appendix B, together with σ_{SW} and λ given by (19). The constants determining the T dependence of these parameters (see Appendix A) are shown in Table II for the LJ fluid. The resulting Z_{LJ} is plotted in Fig. 2 against $\rho^*_{LJ}=\rho\sigma^3_{LJ}$, and compared with MC results from the literature [36]. The agreement is very good over a wide range of T and ρ, and not only at the few states where the mapping equations were solved, but at other states as well.

A more severe test is to analyze the liquid-vapor (LV) equilibrium predicted by the TEOS. Figure 3(a) shows the coexistence densities, and Fig. 3(b) the vapor pressures. Figure 3(a) also includes the densities obtained from the accurate JZG EOS [31]. The TEOS give a good prediction of the coexistence curve except in the proximity of the critical point. The JZG equation provides a much better description of the LV equilibrium, which is not surprising since these EOS are forced to fit the critical point determined by Gibbs ensemble simulation of the LJ system and uses information from about 200 states, whereas in this work we used information at only 12 states. Figure 3(b) compares the vapor pressures of the LJ fluid predicted by the EOS of this work with the simulation results of Lofti, Vrabec, and Fischer [37]. The agreement is seen to be very good. Analysis of the LJ case shows that the mapping method is satisfactory to obtain analytical EOS of simple fluids.

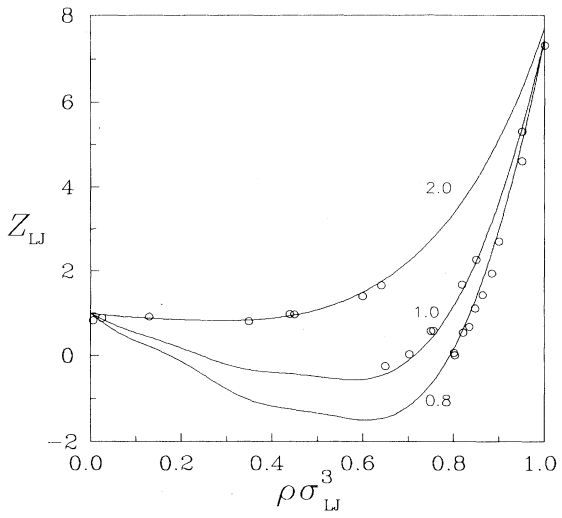

FIG. 2. Compressibility factor Z of the Lennard-Jones fluid from the equation of state of this work (solid lines) at values of T^* as labeled. The circles are Monte Carlo results from Ref. [31].

The behavior of σ_{SW} and λ along the coexistence curve is shown in Fig. 4. At any $T<T_c$ the diameter σ_{SW} is smaller in the liquid than in the vapor (see the discussion above). The attractive range is rather constant for $T/T_c<0.9$: $\lambda\cong 1.43$ in the gas phase and $\lambda\cong 1.7$ in the liquid. It is clear that an exact equivalence between the LJ and SW systems requires quite different diameters σ_{SW} and ranges λ for the liquid and for the vapor branches, except in the proximity of the critical point. The same behavior was found with a purely thermodynamic procedure based on generalized corresponding states [38].

TABLE II. Constants of the parametric approximations to σ^{*3}_{SW} and λ for the Lennard-Jones fluid.

n	B_{0n}	C_{0n}	C_{1n}	C_{3n}	λ_{0n}	α_{1n}	α_{2n}
0	1.180 93	0.920 98	0.117 413	0.034 485	1.739 72	0.055 907 8	1.416 48
1	−0.152 69	−0.026 629 2	−0.336 663	−0.108 758	−0.717 208	0.107 774	14.33
2	0.030 728 9	$2.061\,72\times10^{-4}$	1.215 82	0.031 371 8	0.651 711	−0.028 581 5	−44.0208
3	−0.003 147 7		−0.518 668		−0.231 932		71.9177
4	$1.206\,27\times10^{-4}$						−33.4023

B. EOS for the EXP6 fluids

We turn now to systems for which no explicit EOS are available. An effective $u(r)$ commonly used for modeling real fluids is the EXP6 potential given by

$$u_{\mathrm{EX}}(r)=\frac{\varepsilon}{1-6/\gamma}\left\{\frac{6}{\gamma}\exp[\gamma(1-r/r_m)]-(r/r_m)^6\right\}. \tag{21}$$

Varying γ in (21) changes the repulsive part of $u(r)$: the potential core becomes softer for a smaller γ. Here we consider the cases $\gamma=12$ and 14 which have been used

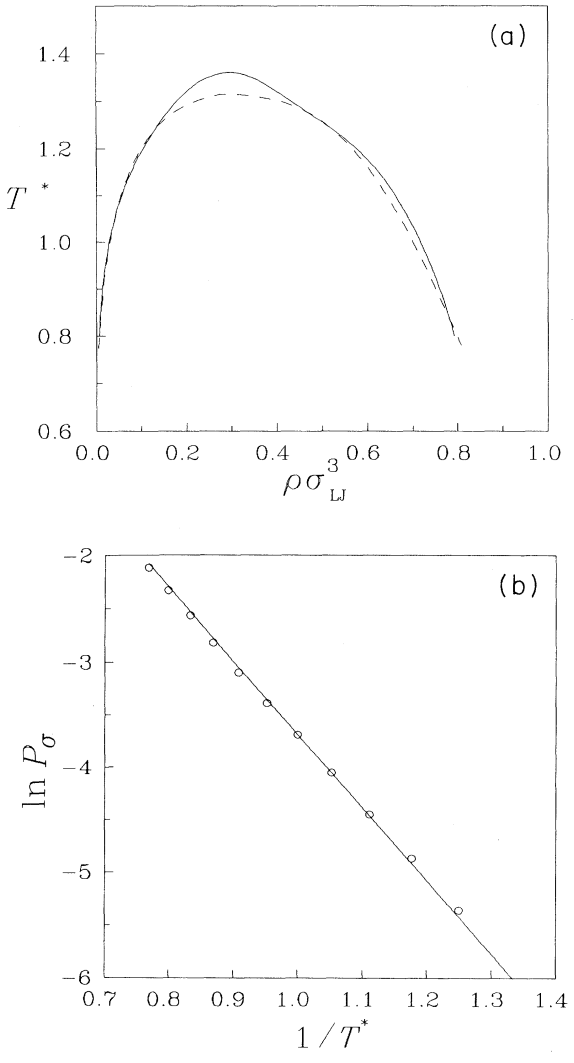

FIG. 3. (a) Coexistence liquid-vapor densities of the LJ fluid as obtained from the equation of state of this work (solid line). The dashed line is the coexistence curve from the JZG equation of state Ref. [32]. (b) Vapor pressures of the LJ fluid. The solid line is obtained from the equation of state of this work, and the circles are Monte Carlo results from Ref. [37].

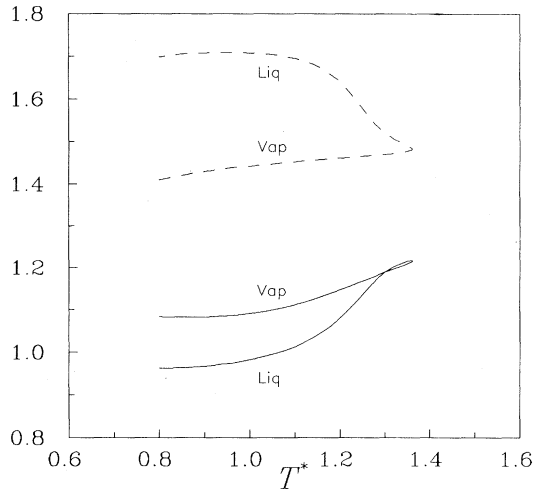

FIG. 4. Equivalent SW diameters σ_{SW} (solid lines) and ranges λ (dashed lines) for the LJ fluid at saturated liquid and vapor densities.

TABLE III. Square-well collision parameters of the EXP6 fluid with $\gamma=12$ and 14 from the RHNC theory.

T^*	$\rho\sigma_X^3$	$\sigma_{\mathrm{SW}}/\sigma_X$	λ	$\rho\sigma_{\mathrm{SW}}^3$
		$\gamma=12$		
1.00	0.005	1.020 36	1.462 30	0.0053
1.00	0.900	1.975 74	1.710 34	0.8361
1.50	0.005	1.002 70	1.516 95	0.0050
1.50	0.300	1.055 56	1.529 01	0.3528
1.50	0.600	1.001 68	1.680 05	0.6030
1.50	0.900	0.966 05	1.730 02	0.8114
2.00	0.005	0.988 65	1.553 75	0.0048
2.00	0.300	1.015 78	1.576 19	0.3144
2.00	0.600	0.986 74	1.696 08	0.5764
2.00	0.900	0.956 24	1.746 02	0.7869
10.0	0.005	0.870 58	1.807 14	0.0033
10.0	0.300	0.872 32	1.831 09	0.1991
10.0	0.600	0.866 12	1.869 40	0.3898
10.0	0.900	0.854 47	1.897 99	0.5615
		$\gamma=14$		
1.00	0.005	1.018 91	1.440 06	0.0053
1.00	0.900	0.976 01	1.696 96	0.8368
1.50	0.005	1.002 27	1.491 94	0.0050
1.50	0.300	1.049 47	1.503 33	0.3468
1.50	0.600	1.005 77	1.652 69	0.6104
1.50	0.900	0.968 13	1.712 66	0.8167
2.00	0.005	0.989 56	1.525 69	0.0048
2.00	0.300	1.015 69	1.545 93	0.3143
2.00	0.600	0.990 75	1.667 37	0.5835
2.00	0.900	0.959 57	1.725 71	0.7952
10.0	0.005	0.887 15	1.743 17	0.0035
10.0	0.300	0.888 91	1.766 69	0.2107
10.0	0.600	0.882 86	1.811 06	0.4129
10.0	0.900	0.871 88	1.846 59	0.5965

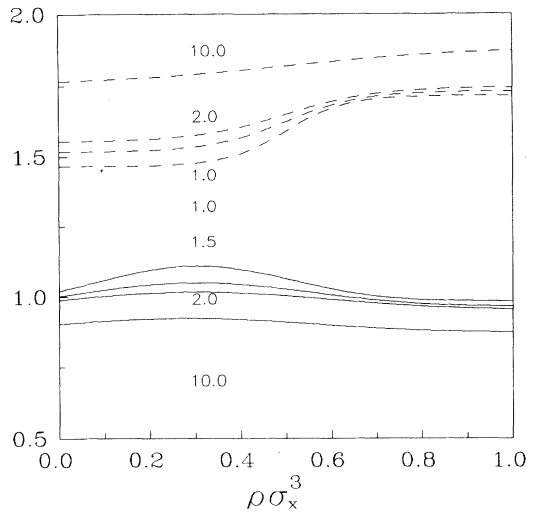

FIG. 5. Equivalent SW diameters σ_{SW} (solid lines) and ranges λ (dashed lines) for the EXP6 fluid with $\gamma=12$ at values of T^* as labeled, except for those at $T^*=1.5$ which carry no labels.

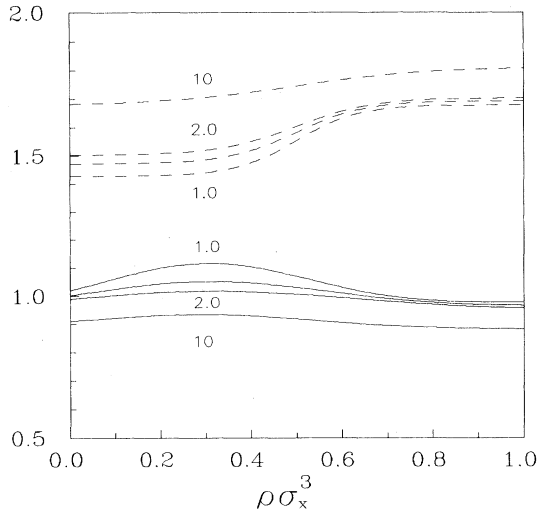

FIG. 6. Equivalent SW diameters σ_{SW} and range λ for the EXP6 fluid with $\gamma=14$. Symbols as in Fig. 5.

for modeling molecular fluids. These two potentials are quite similar, and to be able to discriminate their small differences puts a strong demand on the theory.

Solutions of the mapping equations for the two EXP6 potentials are shown in Table III. The mapping equations were solved with the RHNC integral equation for the EXP6 fluid and with the EOS in Appendix B for the SW properties. Figures 5 and 6 show σ_{SW} and λ in terms $\rho_x=\rho\sigma_x^3$ [where $u_{EX}(\sigma_x)=0$] and $T^*=kT/\varepsilon$, for $\gamma=12$ and 14, respectively. σ_{SW} and λ with ρ and T follow the same trends as for the LJ fluid, and so Eqs. (19) also yield good results. The only change is in a somewhat different temperature dependence of the parameters c_i and α_i (see Appendix A).

TEOS of the two EXP6 fluids are obtained by using the constants for σ_{SW} and λ shown in Table IV. There are no simulations for these fluids to compare with the predictions of this theory, but from the analysis of the LJ case one can safely infer that these EOS provide a good estimate of the EXP6 thermodynamic properties.

The critical properties of the EXP6 fluids, obtained from their TEOS, are given in Table V. The critical temperature is higher for $\gamma=12$ than for $\gamma=14$ because the former potential has a wider attractive well. The effect of γ on the critical and saturated vapor densities is not important. Figure 7(a) shows the saturated liquid densities, and Fig. 7(b) the vapor pressures of the two EXP6 fluids. In both, variables are reduced with the critical values of Table V, and allow us to examine the deviations from corresponding-state behavior. The wider potential well of the $\gamma=12$ fluid produces larger SW ranges λ; see Table III. Hence, as shown in Fig. 7, the $\gamma=12$ fluid has a slightly broader orthobaric. The vapor pressure curve of the $\gamma=12$ fluid has a higher slope than for the $\gamma=14$

TABLE IV. Constants of the parametric approximations of σ_{SW}^{*3} and λ for the EXP6 fluid with $\gamma=12$ and 14.

n	B_{0n}	C_{0n}	C_{1n}	C_{3n}	λ_{0n}	α_{1n}	α_{2n}
				$\gamma=12$			
0	1.065 15	0.602 199	0.125 294	0.047 739 8	1.465 14	0.053 495	1.797 49
1	0.141 327	0.964 508	−0.279 393	−0.133 382	−0.126 524	0.098 425 8	7.212 38
2		−1.178 29	1.071 44	0.057 275		−0.027 122	−1.438 09
3		0.538 141	−0.488 146				
				$\gamma=14$			
0	1.060 60	0.651 344	0.127 667	0.047 052	1.427 28	0.058 357 9	2.448 58
1	0.131 911	0.623 341	−0.206 141	−0.166 862	−0.108 485	0.101 08	8.936 18
2		−0.576 551	0.866 172	0.070 248 7		−0.034 162 6	−4.090 05
3		0.188 139	−0.305 786				

TABLE V. Critical constants of EXP6 fluids with $\gamma=12$ and 14 from their theoretical equations of state.

γ	T_c^*	$(\rho\sigma_X^3)_c$	$(P\sigma_x^3/\varepsilon)_c$
12	1.4823	0.3105	0.1784
14	1.3621	0.3142	0.1745

fluid. This effect on the coexistence properties is systematic and coincides with that found by Fischer *et al.* [39] for the Mie-6 potential:

$$u(r)=\frac{n\varepsilon}{n-6}\left[\frac{n}{6}\right]^{6/(n-6)}[(\sigma/r)^n-(\sigma/r)^6],$$

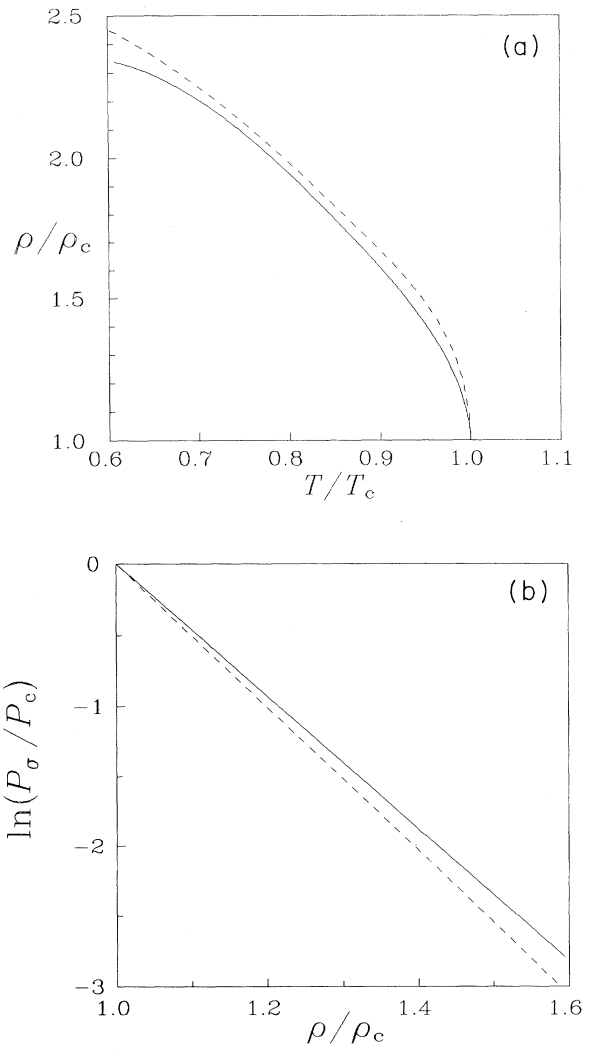

FIG. 7. Effect of γ on the liquid-vapor equilibrium of EXP6 fluids with $\gamma=14$ (solid lines) and 12 (dashed lines) as obtained in this work: (a) saturated liquid densities, and (b) vapor pressures.

where the softness of the core depends on the parameter n.

V. CONCLUSIONS

A method for deriving theoretical EOS of spherical potentials has been developed. We have shown that a given fluid can be mapped into a three-parameter reference system. A family of variable-width SW fluids was found suitable as reference, although other hard-core systems could be used. The known properties of SW fluids, embodied in the SW EOS proposed elsewhere [11,12], are sufficient and accurate enough to solve the mapping equations. When the structure of the fluid of interest is calculated accurately, the mapping equations have unique solutions at all one-phase state points, including the very dense liquid. No evidence of multiple solutions was found, which appeared when a more approximate theory was used.

TEOS of fluids are obtained by solving the mapping equations at a few state points (12 in the cases here considered). The EOS parameters $\sigma_{SW}(\rho,T)$ and $\lambda(\rho,T)$ have a general behavior with ρ and T, and can be represented by parametric functions determined at the few selected state points. These parametric functions plus the SW EOS constitute the TEOS of the fluid. Since EOS are explicit in all variables, they furnish an expedient way for analyzing any thermodynamic property of interest. Further, since $\sigma_{SW}(\rho,T)$ and $\lambda(\rho,T)$ have a kinetic meaning, they contain important information about the system, which allows us to understand the effect of given features of the potential such as, e.g., concern deviations from corresponding-state behavior.

The mapping of the LJ fluid into the SW system was used to test the approach. Considering that information of only 12 states was used, the TEOS derived give good predictions of the pressure and LV equilibrium of the LJ fluid.

The mapping method was applied to fluids with the EXP6 potential with softness parameters $\gamma=12$ and 14. EOS were derived for each system, and the LV equilibria determined. These EOS should have an accuracy similar to the LJ EOS, and can be used confidently to predict the thermodynamics of these fluids. Due to its wider potential well, the fluid with the softer core, $\gamma=12$, has a higher critical temperature and a broader two-phase region.

Extension of this method to fluids with nonspherical potentials and to mixtures is possible and currently being developed. Applications of the mapping method can be easily conceived. If one needs a quick estimate of the EOS and the LV envelope of a fluid model, the whole procedure of solving the mapping equations and obtaining the constants in the parametric equations takes less than a day of work (provided that the software is available). One can also use information obtained from a few simulations to derive EOS in a broad range of temperatures and densities, and to obtain a reasonable estimate of the LV equilibrium and other properties. This is possible because the mapping methodology exploits the knowledge of the EOS of the reference system to build the TEOS of the unknown fluid.

ACKNOWLEDGMENTS

A.G.V. acknowledges the support of the Sistema Nacional de Investigadores and the Consejo Nacional de Ciencia y Tecnología (Conacyt, México). This work was possible thanks to Grant No. 0611-E9110 of Conacyt.

APPENDIX A: PARAMETRIZATION OF THE SW PARAMETERS

1. Determination at constant temperature

The density dependence of the SW diameters is given by Eq. (19a) with $\omega_1=0.30$, $\sigma^*=\sigma_{SW}/\sigma_U$, $\rho^*=\rho\sigma_U^3$, and $\sigma_U=\sigma_{LJ}$ or σ_x. The four parameters c_i are determined by solving (19a) from the values b_0, b_1, b_2, and b_4 of $b(\rho^*)=\sigma^{*3}(\rho^*)$, at the four densities $\rho^*=0$, 0.3, 0.6, and 0.9, respectively. The explicit solution gives, first,

$$c_3=(b_0/b_2-1)/0.6 , \tag{A1}$$

and then one solves the cubic equation for the auxiliary variable ξ:

$$\xi(\xi^2+\xi+1)=\frac{b_3(1+0.9c_3)-b_0}{b_1(1+0.3c_3)-b_0} .$$

Once ξ is determined, the other parameters are given by

$$c_0=\frac{b_0-b_1(1+0.3c_3)}{1-\xi} , \tag{A2}$$

$$c_1=\frac{b_1(1+0.3c_3)-b_0}{1-\xi} , \tag{A3}$$

$$c_2=-(\ln\xi)/0.09 . \tag{A4}$$

The density dependence of the SW ranges is given by Eq. (19b) with $\omega_2=0.52$ (LJ) and $\omega_2=0.50$ (EXP6). The parameters α_0, α_1, and α_2 are obtained from (19b), and the values λ_0, λ_1, and λ_3 of $\lambda(\rho^*)$ at $\rho^*=0$, 0.3, and 0.9, respectively. The solution is

$$\alpha_0=\tfrac{1}{2}(\lambda_3+\lambda_0) , \tag{A5}$$

$$\alpha_1=\tfrac{1}{2}(\lambda_3-\lambda_0) , \tag{A6}$$

$$\alpha_2=\frac{1}{2(0.3-\omega_2)}\ln\left[\frac{\lambda_1-\lambda_0}{\lambda_3-\lambda_1}\right] . \tag{A7}$$

2. Temperature dependence

Once the values of $\{c_i\}$ and $\{\alpha_i\}$ are obtained from Eqs. (A1)–(A4) and (A5)–(A7), at each of the temperatures selected, their temperature dependence was fitted by simple polynomials. For c_1 and c_3 it is given by

$$c_1=c_{10}+c_{11}\beta+c_{12}\beta^2+c_{13}\beta^3 ,$$

$$c_3=c_{30}+c_{31}\beta+c_{32}\beta^2 ,$$

with $\beta=\varepsilon/kT=1/T^*$, but c_0 and B_0 are best fitted with different polynomials for the LJ and the EXP6 fluids. In the first case,

$$c_0=c_{00}+c_{01}T^*+c_{02}T^{*2} \quad (\text{LJ}) ,$$

$$b_0=b_{00}+b_{01}T^*+b_{02}T^{*2}+b_{03}T^{*3}+b_{04}T^{*4} \quad (\text{LJ}) ,$$

and, for EXP6,

$$c_0=c_{00}+c_{01}\beta+c_{02}\beta^2+c_{03}\beta^3 \quad (\text{EXP6}) ,$$

$$b_0=b_{00}+b_{01}\ln\beta \quad (\text{EXP6}) .$$

The temperature dependence of $\{\alpha_i\}$ is represented by

$$\alpha_1=\alpha_{10}+\alpha_{11}\beta+\alpha_{12}\beta^2 ,$$

$$\alpha_0=\alpha_1+\lambda_0 .$$

For the LJ fluid, one has that

$$\lambda_0=\lambda_{00}+\lambda_{01}\beta+\lambda_{02}\beta^2+\lambda_{03}\beta^3 \quad (\text{LJ}) ,$$

$$\alpha_2=\alpha_{20}+\alpha_{21}\beta+\alpha_{22}\beta^2+\alpha_{23}\beta^3+\alpha_{24}\beta^4 \quad (\text{LJ}) ,$$

and, for the EXP6 case,

$$\lambda_0=\lambda_{00}+\lambda_{01}\ln\beta \quad (\text{EXP6}) ,$$

$$\alpha_2=\alpha_{20}+\alpha_{21}\beta+\alpha_{22}\beta^2 \quad (\text{EXP6}) .$$

The constants $\{c_{ij}\}$, $\{b_{ij}\}$, $\{\lambda_{jj}\}$, and $\{\alpha_{ij}\}$ in these equations determine the EOS, and are given in the tables for the potentials considered here.

APPENDIX B: SW EQUATION OF STATE

The main sections of this paper show that the nonconformality of the variable-width SW family is a basic feature in the construction of TEOS. The SW equation of state used here [11,12] is based on the high-temperature expansion of the Helmholtz free energy, following the Barker-Henderson perturbation theory [40]

$$a_{SW}(\rho,\beta,\lambda)=a_{HS}(\rho)+\beta a_1(\rho,\lambda)+\beta^2 a_2(\rho,\lambda)+a_R(\rho,\beta,\lambda) , \tag{B1}$$

where $\beta=\varepsilon/kT$. The term a_{HS} is the free energy of the hard-sphere fluid, taken here from the Carnahan-Starling formula [41]. The mean-field term a_1 can be written as

$$a_1=-4\eta(\lambda^3-1)y_{HS}(\xi) , \tag{B2}$$

where η is the packing function, $y_{HS}(r)$ is the HS background distribution function, and ξ is the mean-value distance $1\le\xi\le\lambda$ (see below). For $y_{HS}(r)$, one uses the expression due to Boublík [42],

$$y_{HS}(x)=\exp(\mu_0+\mu_1\xi+\mu_2\xi^2+\mu_3\xi^3) , \tag{B3}$$

whose coefficients $\mu_i(\eta)$ are given in Ref. [42]. The

TABLE VI. Constants for the mean-field SW equation of state.

m	ξ_{0m}	ξ_{1m}	ξ_{2m}
0	0.773 853	−5.589 61	1.216 473
1	−0.157 937	2.045 30	−2.034 727
2	0.499 370		1.238 574
3	−0.115 220		−0.425 229

mean-value distance ξ is given by

$$\xi=\xi_0+\xi_1\eta+\xi_2\eta^2 ,$$

$$\xi_0=\xi_{00}+\xi_{01}\lambda+\xi_{02}\lambda^2+\xi_{03}\lambda^3 ,$$

$$\xi_1=\frac{6}{\pi}(2-\lambda)\exp(\xi_{10}+\xi_{11}\lambda) ,$$

$$\xi_2=\xi_{20}+\xi_{21}\lambda+\xi_{22}\lambda^2+\xi_{23}\lambda^3 ,$$

where the constants ξ_{ij} are given in Table VI. These values of ξ, substituted in Eqs. (B2) and (B3) reproduce very accurately the simulation data for a_1.

The second order term in (B1) incorporates the exact contributions from the second and third virial coefficients into the macroscopic compressibility approximation. It has the form already used in SW EOS already published [10,12]. The last or residual term in (B1) is an approximation of

$$a_R=\sum_{n=3}^{\infty}\beta^n a_n(\rho,\lambda) ,$$

which also has the correct second virial coefficient, and is a good approximation of the third virial coefficient [10,12].

[1] M. Benedict, G. B. Webb and L. C. Rubin, J. Chem. Phys. **8**, 334 (1940).
[2] T. R. Strobridge, Natl. Bur. Stand (U.S.) Tech. Note **129A**, (1963).
[3] O. Redlich and J. N. S. Kwong, Chem. Rev. **44**, 233 (1949).
[4] D. Y. Peng and D. B. Robinson, Ind. Eng. Chem. Fund. **15**, 59 (1976).
[5] G. Soave, Chem. Eng. Sci. **27**, 1197 (1972).
[6] A. Gil-Villegas, M. Chávez, and F. del Río, Rev. Mex. Fis. **513**, (1993).
[7] F. del Río, Mol. Phys. **76**, 21 (1992).
[8] F. del Río and A. Gil-Villegas, Mol. Phys. **77**, 223 (1992).
[9] P. D. Flemming III and R. J. Brugman, AIChE J. **33**, 729 (1987).
[10] A. Gil-Villegas and F. del Río, Rev. Mex. Fis. **39**, 526 (1993).
[11] A. Gil-Villegas, Ph.D. thesis, Universidad Autónoma Metropolitana, Mexico, 1994.
[12] A. Gil-Villegas, F. del Río and A. L. Benavides, Fluid Phase Eq. (to be published).
[13] K. Aim and I. Nezbeda, Fluid Phase Eq. **12**, 235, (1983).
[14] I. Nezbeda and K. Aim, Fluid Phase Eq. **17**, 1 (1984).
[15] I. Nezbeda and K. Aim, Fluid Phase Eq. **34**, 171 (1987).
[16] G. A. Mansoori, Fluid Phase Eq. **13**, 153 (1983).
[17] Y. Song and E. A. Mason, J. Chem. Phys. **91**, 7840 (1989).
[18] Y. Song and E. A. Mason, Phys. Rev. A **42**, 4743 (1990).
[19] M. A. Hooper and S. Nordholm, Aust. J. Chem. **34**, 1809 (1981).
[20] W. G. Hoover, G. Stell, K. E. Goldmark, and G. D. Degani, Chem. Phys. **63**, 5434 (1975).
[21] L. R. Dodd and S. I. Sandler, Mol. Simul. **2**, 15 (1989).
[22] E. N. Rudisill and P. T. Cummings, Mol. Phys. **68**, 629 (1989).
[23] Y. Rosenfeld and N. W. Ashcroft, Phys. Rev. A **20**, 1208 (1979).
[24] F. Lado, Phys. Lett. A **89**, 196 (1982).
[25] F. Lado, S. M. Foiles, and N. W. Ashcroft, Phys. Rev. A **28**, 2374 (1983).
[26] A. Malijevský and S. Labík, Mol. Phys. **60**, 66 (1987).
[27] A. Malijevský, R. Pospisíl, and S. Labík, Mol. Phys. **61**, 533 (1987).
[28] S. Labík, A. Malijevský, and P. Vonka, Mol. Phys. **56**, 709 (1985).
[29] J. Talbot, J. L. Lebowitz, E. M. Waisman, D. Levesque, and J. J. Weis, J. Chem. Phys. **85**, 2187 (1986).
[30] K. Aim and I. Nezbeda, Fluid Phase Eq. **48**, 11 (1989).
[31] K. J. Johnson, J. A. Zollweg, and K. E. Gubbins, Mol. Phys. **78**, 591 (1993).
[32] T. W. Leland, J. S. Rowlinson, and G. A. Sather, Trans. Faraday Soc. **64**, 1447 (1968).
[33] F. del Río and L. Lira. Mol. Phys. **61**, 275 (1987).
[34] F. del Río, Mol. Phys. **76**, 29 (1992).
[35] J. D. Weeks, D. Chandler, and H. C. Andersen, J. Chem. Phys. **54**, 5237 (1971); **55**, 5422 (1971).
[36] J. J. Nicolas, K. E. Gubbins, W. E. Streett, and D. J. Tildesley, Mol. Phys. **37**, 1949 (1982).
[37] A. Lofti, J. Vrabec, and J. Fischer, Mol. Phys. **76**, 1319 (1992).
[38] E. Fernández-Fassnacht and F. del Río, Rev. Mex. Fis. **33**, 200 (1987).
[39] J. Fisher, R. Lustig, H. Breitenfelder-Manske, and W. Lemming, Mol. Phys. **52**, 485 (1984).
[40] J. A. Barker and D. Henderson, J. Chem. Phys. **47**, 2856 (1967); **47**, 714 (1967).
[41] N. F. Carnahan and K. E. Starling, J. Chem. Phys. **51**, 635 (1969).
[42] T. Boublík, Mol. Phys. **59**, 775 (1986).